Research and Reviews in Materials Science and Chemistry
Vol. 1, Issue 1, 2012, Pages 15-58
ISSN 2319-6920
Pubished Online on October 29, 2012

http://jyotiacademicpress.net

A REVIEW OF DEGRADATION PROPERTIES OF Mg BASED BIODEGRADABLE IMPLANTS

MEHDI RAZAVI[1], MOHAMMADHOSSEIN FATHI[1], OMID SAVABI[2] and MANSOUR BORONI[1]

[1]Biomaterials Research Group
Department of Materials Engineering
Isfahan University of Technology
Isfahan 84156-83111
Iran
e-mail: m.razavi@ma.iut.ac.ir

[2]School of Dentistry
Department of Prosthodontics
and Torabinejad Dental Research Center
Isfahan University of Medical Sciences
Isfahan
Iran

Abstract

Magnesium-based implants have the potential to serve as biocompatible, osteoconductive, and biodegradable implants for load-bearing applications of bone tissue. These implants would be temporarily needed to provide mechanical support during the healing process of injured or pathological tissue. Moreover, the metallic implants, such as pins, screws, and plates for repairing the defects, have to be removed by a second surgery after the bone tissue was healed. Since, the repeated surgery will increases the morbidity and health costs, then, the use of biodegradable metallic implants with a good biocompatibility is expected to

Keywords and phrases: magnesium alloys, biodegradation, biocorrosion, cell culture, bone tissue engineering.

Communicated by Qiuming Peng.

Received May 19, 2012; Revised June 16, 2012

overcome the limitations of conventional metallic biomaterials and remove the second surgery. In spite of the immense potential of biodegradable magnesium alloys, the fast biodegradation rates of magnesium-based implants in the physiological environments impose severe limitations in many clinical applications. Recently, some researches have been done to slow down the biodegradation rate of magnesium alloys. Besides improving the biodegradation rate of magnesium alloys, the biocompatibility should also be considered. This up-to-date review critically summarizes the important recent progresses for controlling the biodegradation rate of magnesium alloys and also mentions to future research trends.

1. Introduction

A variety of metallic biomaterials including titanium alloys, stainless steels, and cobalt-chromium-based alloys have been widely adopted as implant materials [1], because they can be used for load-bearing applications due to their inherent mechanical stability [2]. However, the release of toxic metallic ions or particles by corrosion or wear processes can have undesirable effects on the cells and bone tissues [3]. Moreover, the metallic implants, such as pins, screws, and plates for repairing the defects, have to be removed by a second surgery after the bone was healed [4]. Since, the repeated surgery will increase the morbidity and the health costs, then, the use of biodegradable metallic implants with a good biocompatibility is expected to overcome the limitations of conventional metallic biomaterials and remove the second surgery [5-7].

Magnesium and its alloys are metallic biomaterials that can be biodegradable in the body fluids and also it is an essential element for bone metabolism and may promote the formation of new bone tissue [8, 9]. In addition, the elastic modulus of magnesium is well-matched with that of natural bone, resulting in the reduction of stress shielding effect that can lead to bone loss around the implant [10]. Also, Mg^{2+} is the fourth most abundant cation in the human body and is largely stored in the bone tissues [11, 12]. It is a co-factor in many enzymes, and a key component of ribosomal machinery that translates the genetic information encoded by mRNA into polypeptide structures [13]. Also, early clinical investigations and recent in vitro and in vivo studies suggest that magnesium-based implants have good biocompatibility [14, 15]. It has also been reported that the magnesium-based implants can stimulate

the development of a hard callous at fracture sites [16]. It is worth mentioning that the magnesium alloys possess a density of $1.7–2.0\,g/cm^3$ that is close to that of the natural bones ($1.8–2.1\,g/cm^3$) and the compressive stress and the tensile strength are much higher than those of biodegradable polymers [17]. Compared with the titanium alloys (110–117GPa), the stainless steels (189–205GPa), and the cobalt-chromium alloys (230GPa), the elastic modulus of magnesium alloys (41–45GPa) is closer to that of the natural bones [18].

In the researches of biodegradable magnesium alloys, the crucial problem is the rapid biodegradation rate of magnesium [19-21]. If the implants being made of magnesium alloys are used to repair the diseased bone tissue, they are possible to lose the mechanical stability before the healing of bone tissue due to the rapid biodegradation and also hydrogen gas may collect around the magnesium implants as a result of the fast biodegradation [22, 23]. These factors tend to loosen the connection between the bone tissue and the biodegradable magnesium implants [24]. Recently, some researches have been done to slow down the biodegradation rate of magnesium alloys [25]. Besides improving the biodegradation rate of magnesium alloys, the biocompatibility should also be considered [22].

This up-to-date review critically summarizes the recent progresses for controlling the biodegradation rate of magnesium alloys in the in vitro and in vivo assessments of magnesium alloys for bone tissue engineering applications and future research trends.

2. Biodegradation Mechanism of Magnesium Alloys

The biodegradation of magnesium converts metallic magnesium to the stable ion, Mg^{2+}, in two electrochemical steps, involving the uni-positive ion, Mg^{+}, as an intermediate, as given by Equations (1) and (2). These anodic partial reactions are balanced by the cathodic partial reaction of hydrogen evolution (Equation (3)).

$$\mathrm{Mg} \longrightarrow \mathrm{Mg}^{+} + \mathrm{e}^{-}, \tag{1}$$

(anodic reaction)

$$k\mathrm{Mg}^{+} \longrightarrow k\mathrm{Mg}^{2+} + k\mathrm{e}^{-}, \tag{2}$$

(anodic reaction)

$$(1+k)\mathrm{H_2O} + (1+k)\mathrm{e}^{-} \longrightarrow 1/2(1+k)\mathrm{H_2} + (1+k)\mathrm{OH}^{-}. \tag{3}$$

(cathodic reaction)

The uni-positive ion, Mg^{+}, is reactive, and can react chemically with water. Thus, a fraction, k, of the uni-positive Mg^{+}, reacts electrochemically via Equation (2) to Mg^{2+}, and the complement reacts chemically via Equation (4)

$$(1-k)\mathrm{Mg}^{+} + (1-k)\mathrm{H_2O} + (1-k)\mathrm{OH}^{-} \longrightarrow (1-k)\mathrm{Mg(OH)_2} + 1/2(1-k)\mathrm{H_2}. \tag{4}$$

(chemical reaction)

The overall reaction is given by [15, 25]

$$\mathrm{Mg} + 2\mathrm{H_2O} \longrightarrow \mathrm{Mg(OH)_2} + \mathrm{H_2}. \tag{5}$$

(overall reaction)

3. Common in Vivo and in Vitro Tests of Biodegradable Magnesium Alloys

3.1. In vivo tests of biodegradable magnesium alloys

In vivo tests predominantly perform in small animals, i.e., rats (subcutaneously), guinea pigs, and rabbits [26, 27]. However, an experimental study in sheep reported about the corrosion of magnesium chips in spinal applications [28] and preclinical experiments for cardiovascular stent applications have been performed in pigs [29, 30]. Since the local blood flow and the water content of the different tissues

(local chloride content and hydrogen diffusion coefficient) can be assumed to be different in various animal models, the obtained corrosion rates are not directly comparable. Basically, the obtained different local corrosion patterns due to various anatomical locations or different mechanical loading situations might shed light on the underlying corrosion mechanism of the investigated magnesium alloy in vivo. Dissolved ions from metal implants are always a concern to induce hypersensitivity and allergy. Magnesium alloys AZ31, AZ91, WE43, and LAE442 have been shown to be non-allergenic in an epicutaneous patch test in accordance with the ISO standard [31]. Various analytical methods have been used to determine the elemental components of biodegradable magnesium alloys (Mg, Al, Li, Zn, and rare earth elements) in histological sections, bone, tissue, and body fluids. The application of these methods for trace and ultra trace analysis in often small sample volumes is hampered by several problems. Thus, the sensitivity of the method is mostly in sufficient (SEM-EDX, XRD, XPS, AAS, and XRF) [32, 33].

3.2. In vitro tests of biodegradable magnesium alloys

Investigating of magnesium corrosion has always been a challenge. Corrosion rates of the same magnesium alloy obtained from various corrosion tests exhibit usually different corrosion rates [34]. Thus, in more complex corrosive solutions, which simulate physiological body fluids, the corrosion rate is even more difficult to determine. Therefore, some authors started to measure the volume of hydrogen gas, which evolves with ongoing magnesium corrosion. This simple and inexpensive method has some limitations due to atmospheric pressure changes and possible hydrogen leakages from the experimental set-up [35]. The most common methods to determine the corrosion rate in vitro are immersion tests and electrochemical measurements [36]. The advised guide line for biomaterial testing is the European standard ISO 10993. However, some limitations are conjunct with the use of this standard mainly for testing the biodegradable or corroding biomaterials: (i) the recommended cells are cell lines; and (ii) for biodegradable materials, it is recommended to

prepare extracts and apply these to the cells. One major obstacle is the preparation of extracts from magnesium alloys. The resulting solution, regardless of which alloy is used, shows a high osmolarity and pH and hence exposes the investigated cells to an osmotic shock [37]. For some magnesium alloys, simple test systems such as formazan-based cytotoxicity tests (i.e., MTT, WST-1, XTT) are restricted by the interference between the corrosion and the test agent. Similar problems are also reported for other biodegradable materials such as polymers and calcium phosphates [38, 39]. Thus, a systematic approach to determine suitable in vitro test methods is needed. This in vitro test system should be able to simulate the desired implantation site and its local environment [36]. Table 1 summarizes the common in vitro and in vivo tests of biodegradable magnesium alloys.

Table 1. Common in vitro and in vivo tests of biodegradable magnesium alloys

In vitro tests	In vivo tests
Immersion tests (weight gain, weight loss, corrosion rate) [8-10]	Surgical procedure [18, 65, 71]
Electrochemical tests (tafel polarization, EIS) [28, 52, 54]	Radiographic evaluation [35, 52]
Volume change test [65]	Fluorescent observation [18, 38]
Hydrogen evolution test [53, 73]	Routine pathological examination [17, 45]
pH change test [9, 42]	Immunohistochemistry [33]
Cell culture (attachment, morphology, proliferation, cytocompatibility, and alkaline phosphatase activity) [24, 62]	Microstructural study by using SEM, EDS, XPS, and XRD [56, 62, 68]
Bioactivity tests (SEM-EDX, XRD, AAS) [13, 48, 62]	Analysis of the magnesium ion concentration in blood of implanted samples [49]

4. Control of Biodegradation Rate of Magnesium Alloys via Alloying Elements

Alloying elements play an important role in biodegradable magnesium alloys, and the mechanical properties are usually the primary consideration when introducing alloying elements to the materials. Moreover, in biomedical engineering, factors such as biocompatibility and the rate of biodegradation are crucial. Good biocompatibility is essential in that materials released from the implants to body tissues and fluids must not be toxic, and this is especially important for biodegradable implants. In fact, the large amount of magnesium and potentially harmful alloying elements released during the biodegradation may lead to cytotoxicity, and the degree of toxicity highly depends on the biodegradation rate. Various types of magnesium alloys as well as pure magnesium are proposed for biomedical applications and many in vitro and in vivo studies have been performed to study the biodegradation rate and mechanism. The compositions of representative alloys are summarized in Table 2. Typical examples of Mg-Al-Zn alloys used are AZ91, AZ31, and AZ63. Compared with pure magnesium, the introduction of Al not only modifies the mechanical properties, but also enhances the corrosion resistance [40]. In fact, both $Mg(OH)_2$ and Al_2O_3 will form in a corrosion products layer of Al-containing magnesium alloys during corrosion. $Mg(OH)_2$ is slightly soluble in water and can be transformed into soluble $MgCl_2$ by chloride ions. Unlike $Mg(OH)_2$, Al_2O_3 is insoluble and also cannot be destroyed by chloride ions. So, inclusion of Al can enhance the corrosion resistance of magnesium alloys. Also, an Al concentration that is too high is harmful to neurons and osteoblasts and may be linked to dementia and Alzheimer's disease [41]. Hence, the amount of Al released from the magnesium alloys must be carefully controlled. In vivo studies of the AZ91D magnesium alloy have revealed enhanced osteoblast activity on guinea pig femora. No negative effects have been observed from MG-63

and human-derived cells (HBDC) on AZ91D magnesium alloy in immersion extracts [42, 43]. Mn does not affect the mechanical properties of magnesium alloys significantly, but can increase the yield strength slightly. The most important function of Mn lies in the improved corrosion resistance by converting iron and other metal elements into relatively harmless intermetallic compounds [44]. The poisonous effect of Mn from magnesium alloys on the cell viability and the proliferation has also been observed in [45]. Rare earth (RE) elements can improve the mechanical characteristics, corrosion properties, and creep resistance of magnesium alloys. For example, Y has a high solid solubility in magnesium and is often incorporated into magnesium alloys together with other RE elements to enhance the creep resistance at high temperature. Y has also been reported to benefit corrosion resistance. The use of RE elements in magnesium alloys for biomedical purposes should also be studied from the perspective of their potential cytotoxicity. Hence, it is important to investigate systematically the potential cytotoxicity of dissolved RE elements from biomedical magnesium alloys in the future. Ca contributes to the solid solution and precipitate strengthening. It also acts as a grain refining agent to some extent and additionally contributes to grain boundary strengthening. Zn improves the strength of magnesium alloys, owing to solid solution strengthening and castability [46]. Zn and Ca are both biologically elements, and Zn- and/or Ca-containing magnesium alloys such as Mg-3Zn, Mg-1Zn-1Ca, and Mg-5Ca have been proposed as candidates for biodegradable implants [47-49]. In the Mg-Ca system, Mg_2Ca is the only second phase besides α-Mg and distributes around grain boundaries. Good cell attachment has also been observed from Mg-Zn, Mg-Ca, and Mg-Zn-Ca alloys according to direct cell cultures [50].

Table 2. Common biodegradable magnesium alloys

Family	Alloys	Alloying elements		
Pure Mg	Mg [14]			
Mg-Al-Zn	AZ31 [32]	3Al	1Zn	
	AZ63 [18]	6Al	3Zn	
	AZ91 [53, 56]	9Al	1Zn	
Mg-Ca	Mg-*x*Ca (*x* = 1, 2, 3, …) [36, 62]	*x*Ca		
Mg-Zn-Ca	Mg-1Zn-1Ca [8, 46]	1Zn	1Ca	
Mg-Zn-Mn-Ca	Mg-2Zn-1.2Mn-1Ca [63]	2Zn	1.2Mn	1Ca
Mg-Si-Ca		1Si	1Ca	
Mg-Zn	Mg-*x*Zn (*x* = 1, 3, 6, 10) [48]	*x*Zn		
Mg-Zn-Mn	Mg-1Zn-1Mn [25, 53]	1Zn	1Mn	
Mg-Mn	Mg-1Mn [32]	1Mn		
RE containing magnesium alloy	LAE442 [16]	4Li	4Al	2RE
	WE43 [71]	4Y	3RE	
	ZE41 [43]	4Zn	1RE	
	AE44 [28]	4Al	4RE	
	Mg-*x*Gd (*x* = 5, 10, 15, …) [32]	*x*Gd		
	WZ21 [26]	2Y	1Zn	
	Mg-8Y [31]	8Y		

Kirkland et al. [50], have been studied a number of magnesium alloys with biomedical grade to provide a ready reference. They have presented a survey of data for biodegradation rates of experimental magnesium alloys that reveal: It is possible to produce magnesium alloys of customized biodegradation rates-based on corrosion specific. The results show that the mass loss rates of the various magnesium alloys vary over a range of 3 orders of magnitude (Figure 1). This is a remarkable result in its own right, and reflects a very unique trait of magnesium alloys, in that alloying can have a major impact on the subsequent rates of reaction. To aid in the interpretation of the results herein, the mass loss data rates were converted to a penetration in mm/yr. These results are useful in assessing the notion that some alloys can dissolve at extremely

high rates, such as many tens of mm/yr. Such high rates are assumed to be too rapid for the purposes of most implant materials. It should be noted that the selection of alloys in Figure 1 has been done on the basis of potential for biocompatibility, with alloying elements such as Mn, Fe, Ni, Au, Ag, etc. [50].

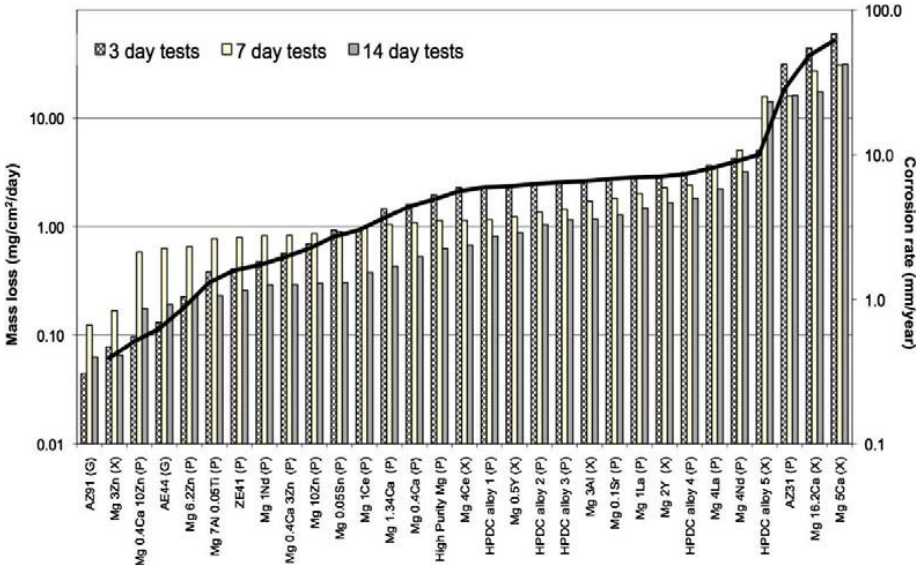

Figure 1. Experimentally determined corrosion rates for magnesium alloys tested herein. The notation 'G' refers to alloys, which suffered a general corrosion mode; 'P' refers to a pitting corrosion mode; and 'X' refers to extremely localized corrosion. Reproduced from Kirkland et al. [50] with kind permission.

5. Control of Biodegradation Rate of Magnesium Alloys via Heat Treatment

In fact, chemical heterogeneity caused by crystallization, precipitation, and segregation during the casting process can have a negative impact on the surface corrosion resistance, and it can also decreases the homogeneous degradation of magnesium alloy. Heat treatments can cause microstructural changes and redistribution of metal elements. A

homogeneous structure and so a homogeneous degradation rate can be obtained by a solution aging process [34]. A solution treatment at 413ºC causes microstructural evolution involving four processes: Dissolution of the β phase, formation of a fine-grain structure, morphological change of the globules into a traditional grain shape, and grain coarsening. During aging at 216ºC, discrete precipitates are preferentially initiated at some of the grain boundaries and then interconnected precipitates emerge inside the grains with accelerated age-hardening kinetics. These microstructural changes can affect selected properties of the magnesium alloys. Some researchers have found that a solution treatment decreases the amount of second phase particles inside the grains and weakens strong pinning on dislocations [23]. It has been reported that the secondary phase has an effect on the corrosion resistance and homogeneous degradation rate of aluminum-containing magnesium alloys [27, 31]. The β phase plays dual roles that depend on the amount and distribution of this phase. A fine and homogeneous phase appears to be a better anti corrosion barrier. Otherwise, the presence of the β phase in the alloys could deteriorate the corrosion performance as it can act as an effective galvanic cathode. The beneficial effect of the β phase on the corrosion properties may be enhanced by grain refinement. The influence of the solution and aging treatment on the corrosion resistance of biomedical magnesium alloys in a simulated body environment has been seldom probed. From a practical point of view, it is important to know the effects of the suitable heat treatment on the biodegradation rate in an in vitro environment. Better understanding of the process and mechanism can improve the biodegradation rate of magnesium alloys in a biological medium thereby expediting the acceptance and use of the biodegradable materials in biomedical implants. In order to investigate the effect of heat treatment on the biodegradation behaviour of magnesium alloys, Liu et al. [51], heat treated the magnesium alloy according to Table 3.

Table 3. Heat treatment parameters. Reproduced from Liu et al. [51] with kind permission

	#1	#2	#3	#4
Solution Treatment	Untreated	413°C, 24h	413°C, 24h	413°C, 24h
Aged treatment	Untreated	216°C, 1h	216°C, 5.5h	216°C, 12h

Figure 2 shows the variation of the magnesium ion concentration and pH as a function of the immersion time. It is interesting to note the relative changes in the pH and magnesium dissolution rates after different exposure time. The magnesium ion concentration measured from sample 1 is greater than those of the aged samples at each testing time point, indicating a greater corrosion rate. As a bulk material, the phase constituents and their distribution as well as the grain size affect the corrosion properties significantly. AZ magnesium alloys are typically composed of a matrix of α grain with the β phase (the intermetallic $Mg_{17}Al_{12}$) along α grain boundaries [17]. In a chloride solution, the corrosion performance of AZ alloy is determined by the β fraction, the continuous β phase around α grains and porosity. The amount and distribution of the β phase (discontinuous precipitation, (DP) and continuous precipitation, (CP)) determine the corrosion performance of the magnesium alloy. It has been found that a solution or aged treatment can effectively change the distribution and amount of the β-$Mg_{17}Al_{12}$ phase [7]. Figure 2(b) indicates that the pH value rises initially and then decreases. Since, the $Mg(OH)_2$ film can inhibit corrosion of the magnesium alloy to some extent [4], then, the pH value decreases. Thus, according to researches done by Liu et al. [51], the solution treatment at 413°C for 24h followed by aging at 216°C for up to 1h leads to complete dissolution of the β phase into the α phase grains causing the formation of new well defined α grains with sharp grain boundaries. The β-$Mg_{17}Al_{12}$ precipitates form after 5.5h of aging, and the amount and

distribution become greater and wider with longer aging time. With increasing the aging time, the treated alloys show greater corrosion resistance. After 14 days immersion in simulated body fluid, the lowest corrosion rate achieved is about 1/2 of that of the untreated alloy. The change in the microstructure is thus shown to impact the corrosion behaviour of the alloys. For the aged materials, shallow filiform and pitting corrosion is observed. In comparison, deep and uniform corrosion is observed on the untreated magnesium alloy [51].

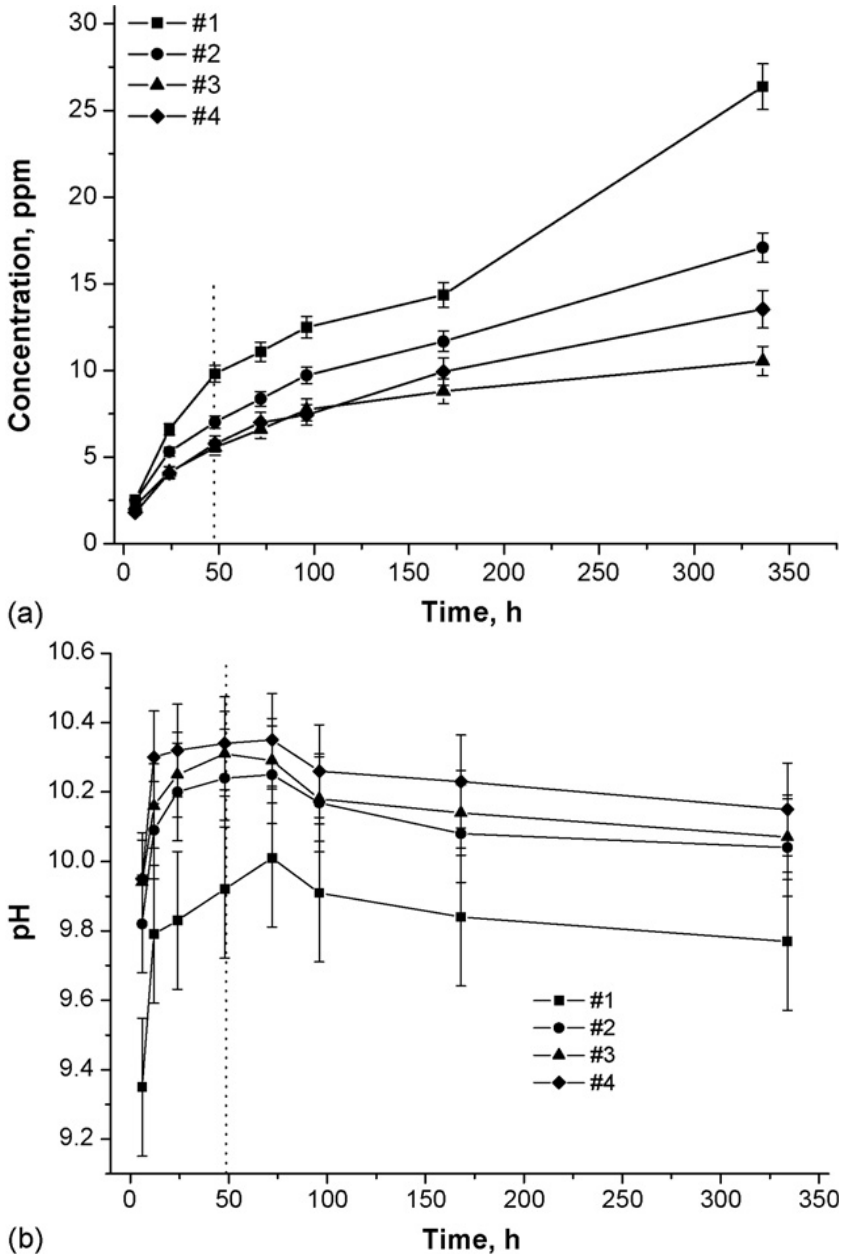

Figure 2. Changes in of Mg ion concentration and pH as a function of immersion time: (a) Mg ion concentration; and (b) pH value. Reproduced from Liu et al. [51] with kind permission.

6. Control of Biodegradation Rate of Magnesium Alloys via Grains Refinement

Wang et al. [46], investigated the biodegradation behaviour of the squeeze cast (SC), hot rolling (HR), and equal channel angular pressing (ECAP) samples under simulated physiological conditions. The weight loss after a preset number of days of immersion has been measured for all three materials. The results are plotted in Figure 3. The degradation process, starting off with a high degradation rate, is seen to slow down with the immersion time. The retardation of the degradation process with time stems from the accumulation of the corrosion products on the specimen surface. Beside the main corrosion products, magnesium hydroxide, and other magnesium phosphates and carbonates are also produced. They form a layer on the surface of the sample, retarding the corrosion process [9, 10]. While the degradation behaviour for all three material conditions (SC, HR, and ECAP) show a similar qualitative trend, with the corrosion rate decreasing with the immersion time, significant quantitative differences in their degradation kinetics are obvious. SC samples exhibit a much higher degradation rate than the material in the other two conditions. The degradation rates of the HR and ECAP samples are initially different, but after the first two days, practically no difference in the degradation rate is observed. The reduced corrosion rate of magnesium alloy by HR treatment must be associated with the grain refinement effect. A further reduction of the grain size by ECAP did not lead to a decrease in the corrosion rate. The reasons for that, and the possible role of the dislocations and vacancies produced by ECAP, are yet to be investigated. Grain refinement by hot rolling has been shown to lead to a significant enhancement of fatigue life and endurance limit, as well as a reduction in corrosion rate. While fast corrosion kinetics is generally beneficial in the biodegradable implants, the corrosion rate achieved with candidate magnesium alloys is too high for their use for surgical applications. Hot rolling and grain refinement provide a desirable retardation of corrosion [46].

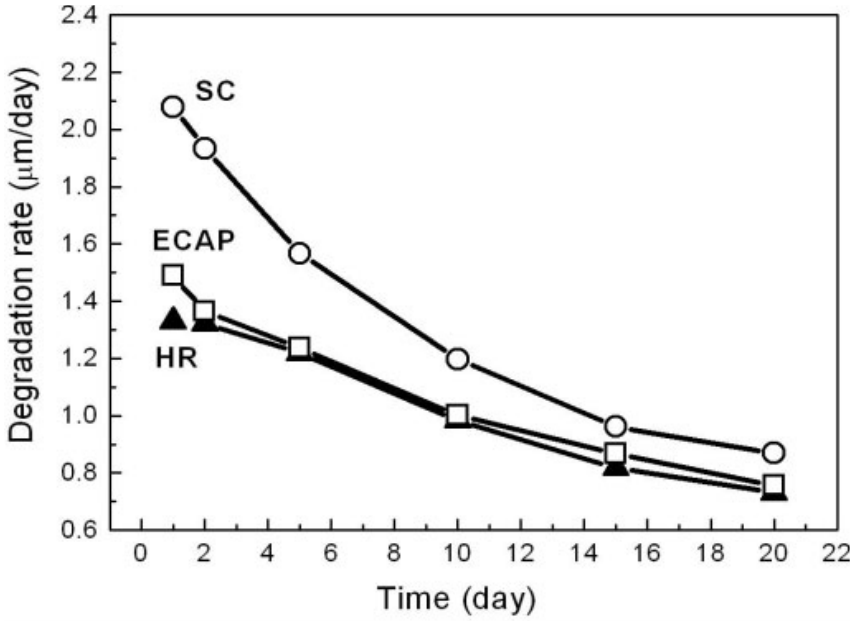

Figure 3. Degradation rate of SC, HR, and ECAP samples in Hank's solution under static conditions. Reproduced from Wang et al. [46] with kind permission.

7. Control of Biodegradation Rate of Magnesium Alloys via Coating Progresses

7.1. Polymer-based coating

7.1.1. Polycaprolactone (PCL) coating

Wong et al. [43], improve the properties of magnesium implants via the deposition of a biodegradable polymer-based porous membrane made of polycaprolactone (PCL) onto a commercially available magnesium alloy in order to control its biodegradation rate. The addition of the polymeric membrane was found to reduce the degradation rate of magnesium. Three rabbits have been used in this study. Each rabbit has been implanted with either of HPM (high porosity membrane) coated, LPM (low porosity membrane) coated or uncoated samples, whereas two samples have been implanted into each rabbit (as shown in Figure 4) [43].

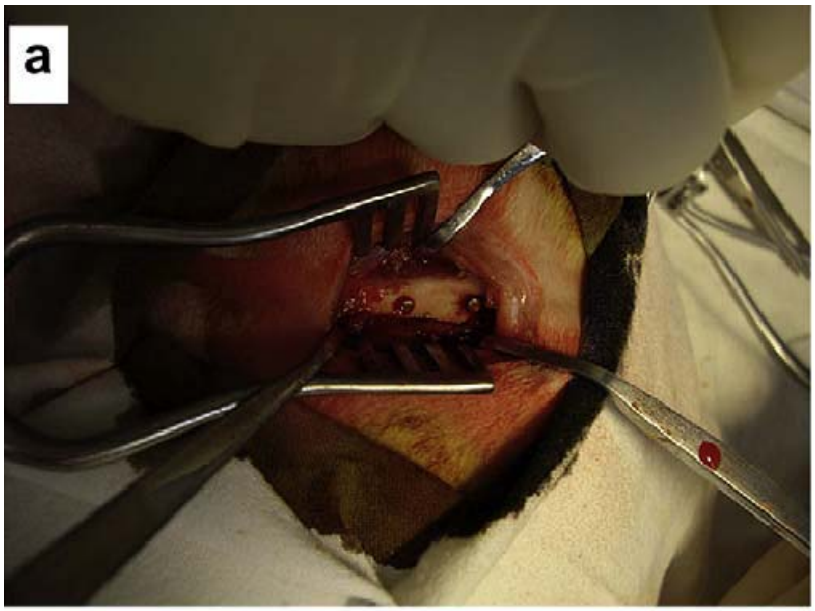
a


b

Figure 4. Uncoated and PCL-coated sample rods implantation in greater trochanter of New Zealand white rabbit for 2 months: (a) uncoated, (b) LPM, and (c) HPM. Reproduced from Wong et al. [43] with kind permission.

Figure 5 shows the tissue response to both polymer-coated and uncoated magnesium alloy after 2 months of implantation, where new bone tissue (black arrows) are observed to form around the implant. All samples show direct contact with the newly formed bone. Osteoblasts, which are responsible for the new bone formation, are also observed around the implants (green arrows). More bone has formed around the polymer-coated implants in comparison to the uncoated sample. Histological analysis reveals an area of bone formation around the implants, although corrosion is found on uncoated and HPM samples in the histological staining. There is an absence of inflammation and necrosis, which suggest that there are no toxic effects in the surrounding tissues. This is a good indication that the coated sample would be safe for in vivo use, considering that once the polymer membrane degraded, the

uncoated magnesium alloy would also degrade and not induce adverse effects into the localized tissues. However, upon comparison of the amount of new bone formation, it is found that the uncoated sample has the least amount of new bone formation and the polymer-coated samples have the new bone volume in descending order of LPM > HPM. Higher amounts of bone formation around the polymer-coated samples as compared to the uncoated samples may be due to several reasons. One reason for this may be attributed to a reduced rate of corrosion, as the polymer-coating decreased the amount of direct contact with the body. In addition, large amounts of magnesium ion release during corrosion of the uncoated sample possibly inactivate new bone formation [51], thereby resulting in less new bone formation around the uncoated sample when compared to the polymer-coated samples. The high levels of new bone formation found on the LPM sample may be explained by the release of low levels of magnesium ions, which has been reported to enhance osteoblastic activity and thus generate a stimulatory effect on the growth of new bone tissue. Hence, LPM-coated samples may have induced more new bone formation due to the release of low levels of magnesium ions [43].

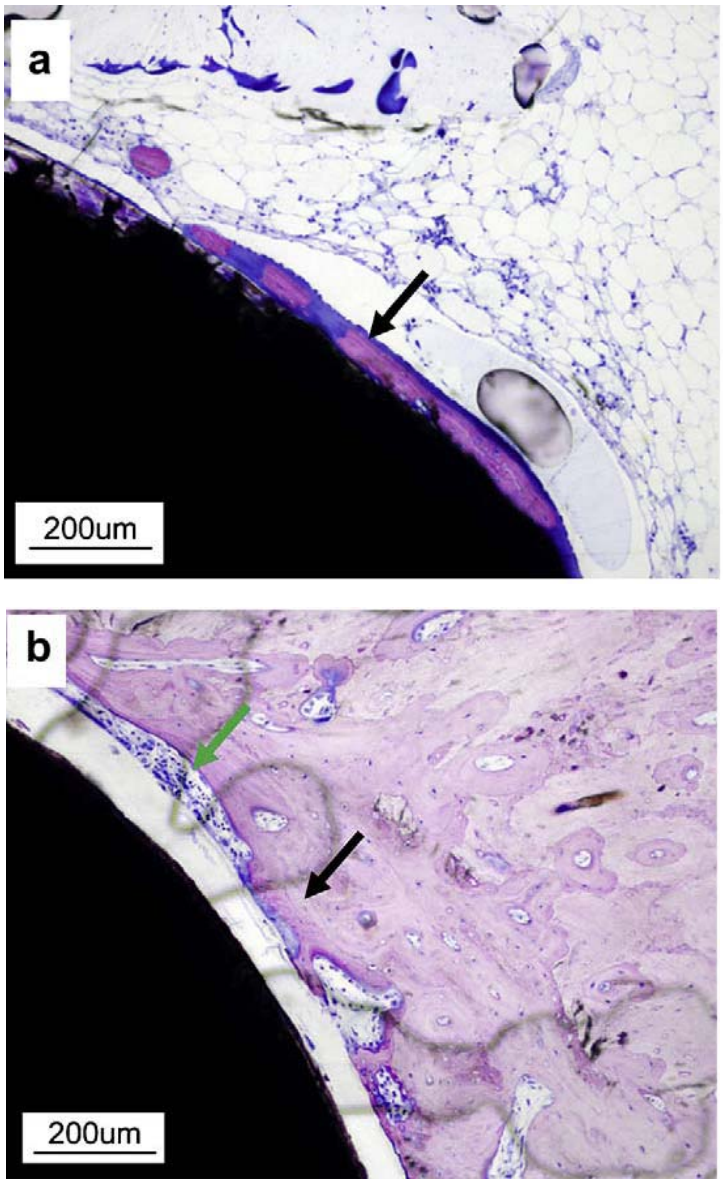
a
200um
b
200um

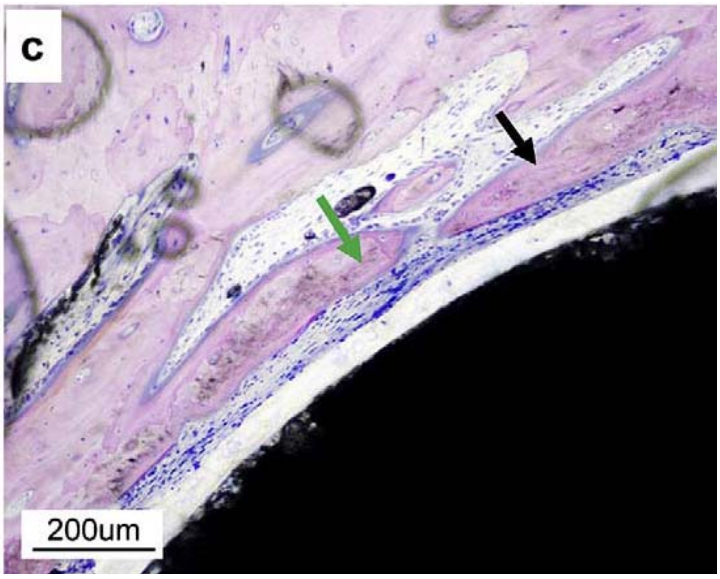

Figure 5. Histological photographs of gimesa stained of the bone tissue formed around the implant after 2 months' implantation in the greater trochanter, where arrows represent the newly formed bone and circles represent the presence of osteoblasts: (a) uncoated, (b) LPM, and (c) HPM. Reproduced from Wong et al. [43] with kind permission.

The electrochemical polarization curves of the PCL samples are shown in Figure 6. The corrosion potential (E_{corr}) shows that the polymer-coated magnesium alloys shifted the open circuit potential to a more positive potential. Therefore, both the E_{corr} and I_{corr} show that the PCL coated samples are able to enhance the corrosion resistance of magnesium alloy [43].

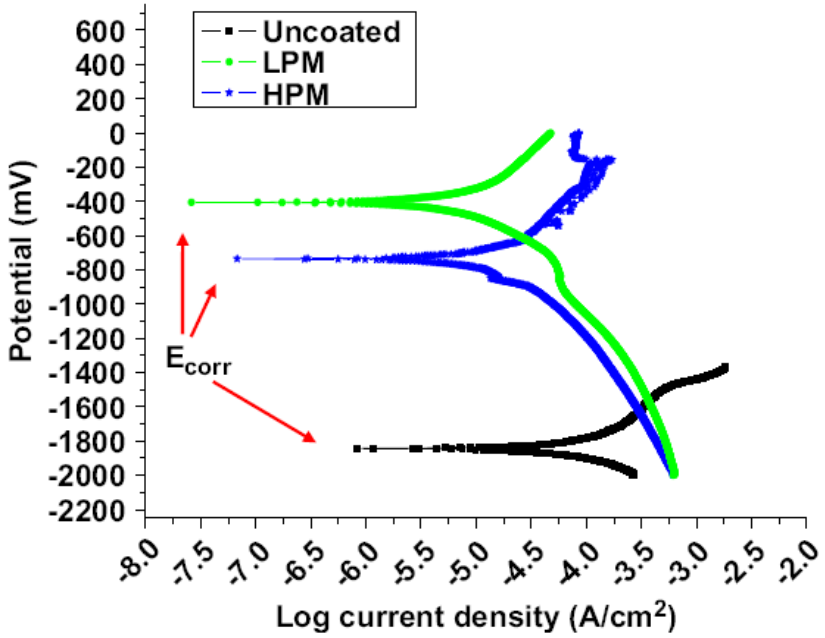

Figure 6. Potentiodynamic polarization curves of PCL-coated and uncoated magnesium alloys, which was obtained from the electrochemical measurement. Reproduced from Wong et al. [43] with kind permission.

Figure 7 shows the viable cells on the uncoated and polymer-coated samples after 1 and 3 days of cell culture. On day 1, focal adhesion and cells spreading are observed on the polymer-coated samples (Figure 7(a)), while no cell attachment is observed on the uncoated sample. After 3 days of cell culture (Figure 7(b)), the osteoblasts exhibit good cell spreading and have almost grown to 100% confluency on the polymer-coated samples, in contrast to the uncoated sample, which had no cell growth [43].

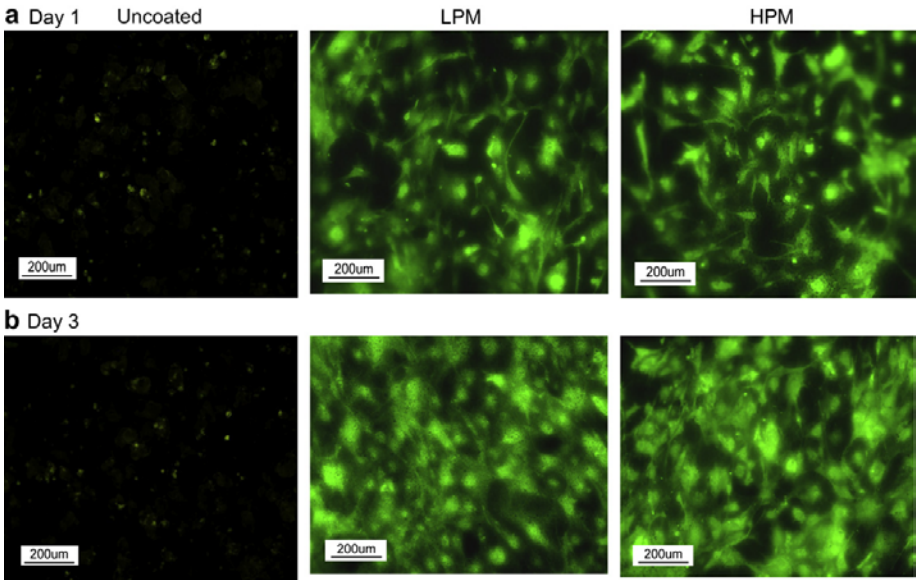

Figure 7. Microscopic views of GFP mouse osteoblasts cultured on PCL-coated and uncoated AZ91 magnesium alloy after 1 and 3 days: (a) 1 day; and (b) 3 days. 5000 GFPOB were cultured on the coated and uncoated samples for 1 and 3 days so as to evaluate the cytocompatibility of the polymer-coated magnesium alloys. Reproduced from Wong et al. [43] with kind permission.

Thus, the in vitro studies indicate good cytocompatibility osteoblast cells with the polymer-coated samples, which are not observed for the uncoated samples. The in vivo study indicates that the uncoated sample degraded more rapidly than that of the polymer-coated samples. Although new bone formation is found on both samples, higher volumes of new bone are observed on the polymer-coated samples. Collectively, these data suggest that the use of polymeric membrane may be potentially applied for future clinical use [43].

7.2. Bioceramic-based coating

One of the effective measurements to reduce the biodegradation rate of magnesium alloys is the surface modification [52, 53]. For the biomaterials, a surface coating is also an effective way to improve the surface bioactivity [54]. Therefore, it is possible to reduce the

biodegradation rate of magnesium alloys and improve the surface bioactivity by selecting a proper surface modification [55]. The surface modification of magnesium alloys will improve the biocompatibility of these alloys by reducing the biodegradation rate and inducing the better bone-implant interfaces [56]. Since, the rapid biodegradation rate of magnesium alloys could possibly lead to the appearance of a gap at the interface between the implant and the surrounding bone tissue, as described in Figures 8(A)-(B), then, the bioactive bone-like apatite coating is considered to reduce the biodegradation rate and simultaneously to ameliorate the interfacial biocompatibility. The principal model is explained briefly in Figures 8(C)-(D). Accordingly, the ideal case is, on one hand, the bioactive coating can enhance the cellular biocompatibility to form the new bone that mixed with the biodegradation products. On the other hand, the released ions during the biodegradation can induce the new bone formation at the opposite interface of host bone. Meanwhile, the coating decreases the biodegradation rate of implant. Therefore, the new bone formation that described above can have enough time and amounts to produce the strong chemical bond [57].

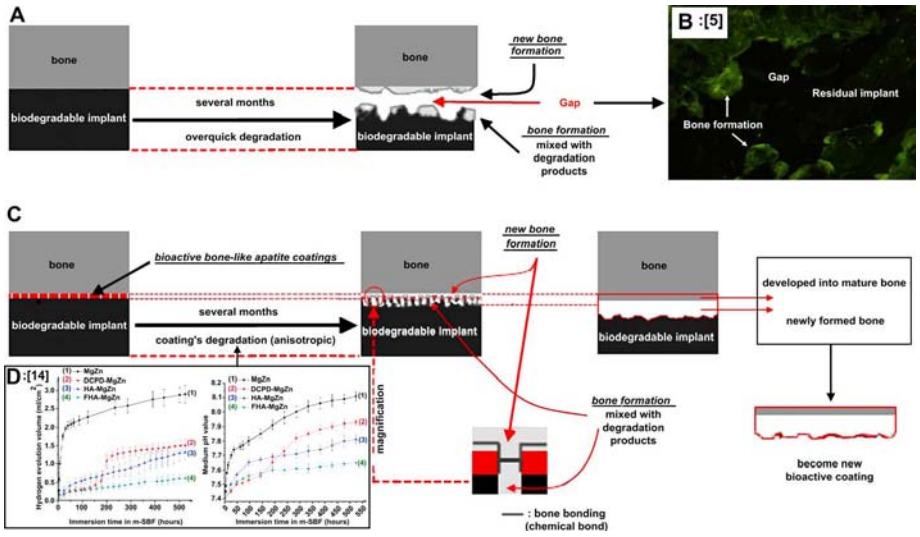

Figure 8. The model that explains the improvements taken by the bioactive bone-like apatite coatings. (A) The relatively rapid degradation rate of magnesium may possibly lead to the appearance of the gap at the interface. (B) The typical tetracycline label 14 weeks post-operation. (C) The bone-like apatite coating can reduce the degradation rate and simultaneity to ameliorate the interfacial biocompatibility. (D) The corrosion protective effects of the coatings got by testing the H_2 releasing rate and the pH value changes. Reproduced from Li et al. [57] with kind permission.

7.2.1. Calcium phosphate (Ca-P) coating

Bioactive coatings such as calcium phosphates are important for the surface modification of implanted devices [58], and have been successfully applied in order to promote the direct attachment of surrounding hard tissue and to suppress the release of corrosion products into the human body [59].

Xu et al. [53], coated the calcium phosphate on a magnesium alloy by a phosphate treatment in order to improve the surface bioactivity of magnesium alloy.

Figure 9 shows the morphology of cells that cultured for 5 days on the surface of (a) the naked magnesium alloy and (b) the calcium phosphate coated magnesium alloy. The cells on the surface of naked magnesium alloy maintained a round or spindle-like morphology during the whole incubation period. In contrast, for calcium phosphate coated magnesium alloy, the cells are sail-like, elongated, and thicker in the central area of nucleus and flattened in the peripheral regions. Some cells have spread across the surface and contacted with each other. Also, the cells and the excreted matrices have been connected together and it is hard to distinguish between the cells and matrices [53].

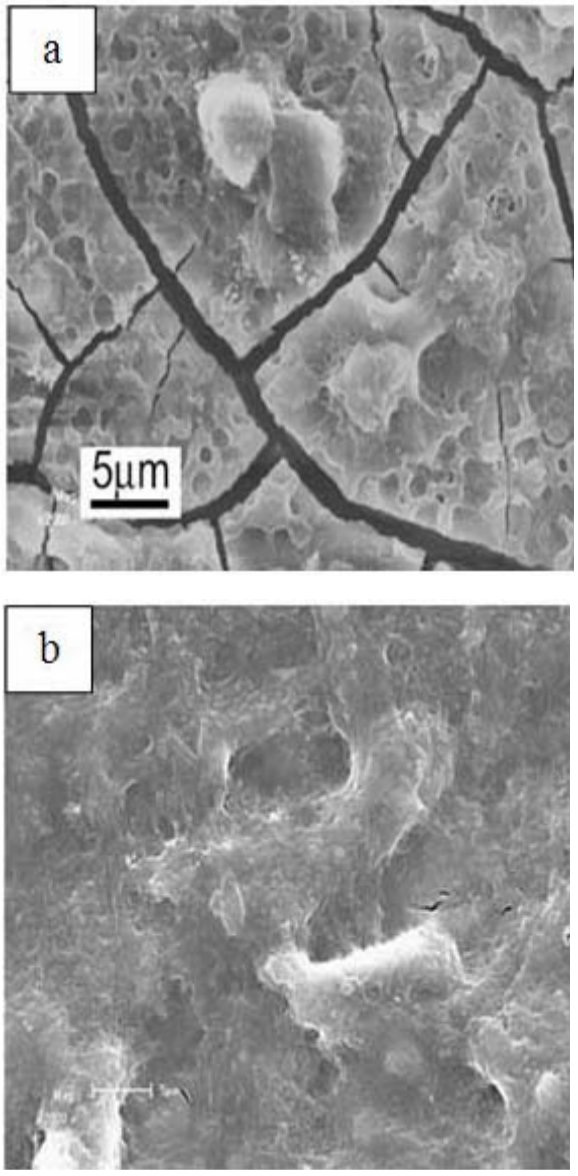

Figure 9. The morphology of the cells cultured for 5 days on the surfaces of (a) the naked magnesium alloy and (b) the calcium phosphate coated magnesium alloy. Reproduced from Xu et al. [53] with kind permission.

Figure 10 shows the cell proliferation on different samples. According to Figure 10, the cell number increases with increasing the culture time, indicating that a cell could attach and proliferate on the surface of samples. For the naked magnesium alloys, there is no evident increase in the cell number at all time intervals ($p > 0.05$), indicating that the naked magnesium alloy does not promote the cell growth and proliferation. In comparison with the naked magnesium alloy, the cell number on the surfaces of calcium phosphate coated magnesium alloy and pure titanium have shown a significant increase at all time intervals, indicating that both the calcium phosphate coated magnesium alloy and pure titanium have a significantly better surface bioactivity compared to the naked magnesium alloy [53].

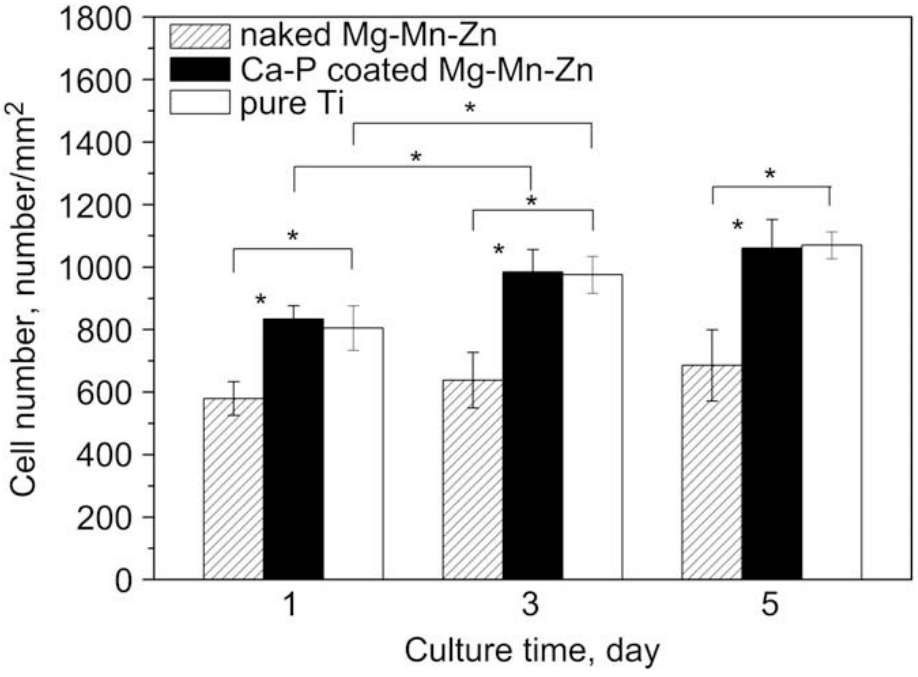

Figure 10. Growth of L929 cells versus culturing time on the naked magnesium sample, the calcium phosphate coated sample and the pure titanium sample ($^{*}p < 0.05$). Reproduced from Xu et al. [53] with kind permission.

The fluoroscopic images of bone and magnesium alloy implants after 4 weeks implantation are shown in Figure 11. It can be seen that the new osteoid tissue has formed around both the naked magnesium alloy implant (Figure 11(a)) and calcium phosphate coated magnesium alloy implant (Figure 11(b)). Compared to the naked magnesium alloy implant, the newly formed osteoid tissue around the calcium phosphate coated magnesium alloy implant is compact and uniform. In addition, the outline shape of magnesium implants has slightly changed, indicating that the implants have been corroded by the body fluid, or the implant have been degraded in the body. However, it is hard to distinguish the difference in the degradation between the naked magnesium alloy implant and calcium phosphate coated magnesium alloy implant after 4 weeks implantation because the duration is not long enough to evaluate the in vivo degradation. According to the fluorescent observation, more new osteoid tissues, which are compact and uniform, are observed around the calcium phosphate coated magnesium alloy implant than around the naked magnesium alloy implant after 4 weeks implantation, indicating that the calcium phosphate coated magnesium alloy implant is more compatible and bioactive for bone growth at the early healing process [53].

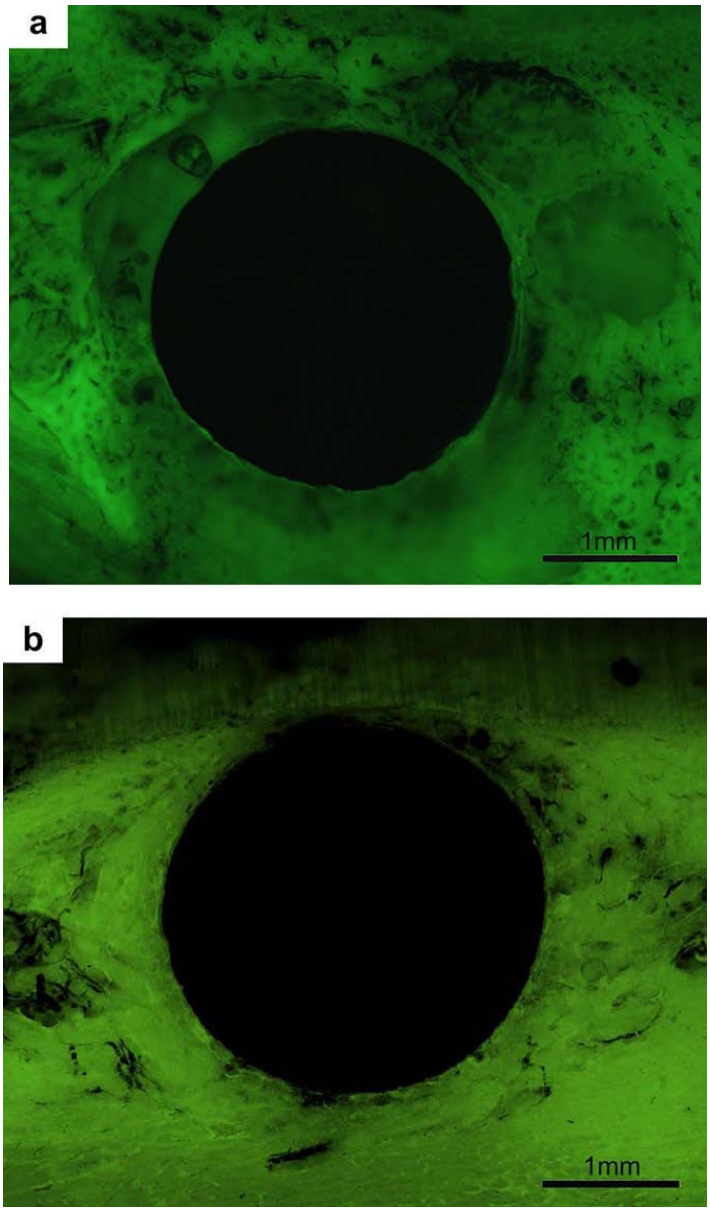

Figure 11. Fluoroscopic images of the cross-section of (a) a naked magnesium implant and (b) a calcium phosphate coated magnesium implant after 4 weeks implantation (the dark area is magnesium implant). Reproduced from Xu et al. [53] with kind permission.

Figure 12 shows one naked magnesium alloy (left) and one calcium phosphate coated magnesium alloy (right) rod sample, which have been implanted into the left femoral shaft of a rabbit. According to Figure 12, the calcium phosphate coated magnesium alloy rod sample with white colour has not corroded. In contrast, the naked magnesium alloy sample with the black colour has corroded. Because the corrosion of magnesium alloys is accompanied by formation of magnesium hydroxide layer with black colour on the surface [53].

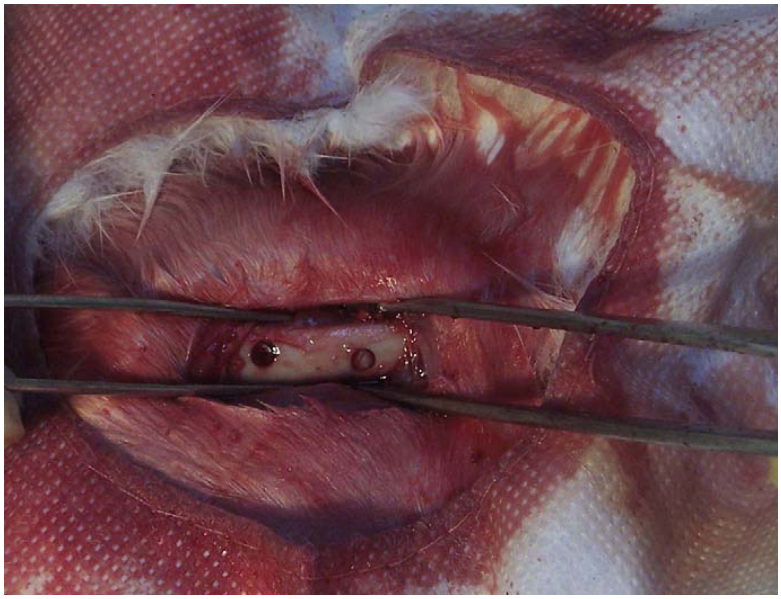

Figure 12. One naked magnesium alloy (left) and one calcium phosphate coated magnesium alloy (right) rod sample, which have been implanted into the left femoral shaft of a rabbit. Reproduced from Xu et al. [53] with kind permission.

Thus, the calcium phosphate coating is also beneficial for cell adhesion and growth. In vitro cell tests demonstrate that the calcium phosphate coating provides the magnesium alloy with a significantly better surface cytocompatibility and the in vivo results also confirm that the calcium phosphate coating exhibit significantly improved osteoconductivity and osteogenesis in the early first 4 weeks postoperation period [53].

7.2.2. Hydroxyapatite (HA) coating

The hydroxyapatite $[HA: Ca_{10}(PO_4)_6(OH)_2]$ coating can satisfy dual properties. The hydroxyapatite is a major inorganic component of the natural bone and can accelerate the bone growth [60]. But the mechanical strength of hydroxyapatite is too poor to be used in the load bearing applications [61]. Therefore, the hydroxyapatite coating has been deposited on the surface of metallic implants to improve the biocompatibility and bioactivity [62].

Song et al. [63], produced the bioactive hydroxyapatite coating by electrodepostion method to improve the biodegradation behaviours of magnesium alloys in the human body environment.

Figure 13 shows the potentiodynamic curves and EIS plots of magnesium alloy with and without the hydroxyapatite coating in the SBF solution. From the potentiodynamic curves, it can be seen that the corrosion current density for magnesium alloy substrate increases quickly at the beginning of anodic side. Then, the diffusion-controlled anodic current behaviour is observed at the end of curves due to the fast corrosion rate [63]. It is indicating that the magnesium alloy substrate suffers severe attack in the SBF solution [64]. This result shows that the hydroxyapatite coating can prevent the magnesium alloy from the biodegradation. Additional, the free corrosion current for the hydroxyapatite coating is almost ten times lower than that of the magnesium alloy substrate. Thus, it implies that the hydroxyapatite coating improves the biodegradation property of magnesium alloys in the SBF solution. According to the EIS plots, obvious changes can be found due to the presence of hydroxyapatite coating. The magnesium alloy substrate exhibits two capacitance loops at the high frequency and low frequency, respectively [63]. The high frequency capacitance loop describes the characteristics of electric double layer. The low frequency loop is related to the adsorption of corrosion products on the magnesium alloy surface [65]. The plot for hydroxyapatite coating only contains one capacitance loop, which implies that the coating was undamaged. Additional, the capacitance loop diameter of the hydroxyapatite coating is bigger than that of the magnesium alloy substrate. Thus, the hydroxyapatite coating can reduce the biodegradation rate of magnesium alloy in the SBF solution [63].

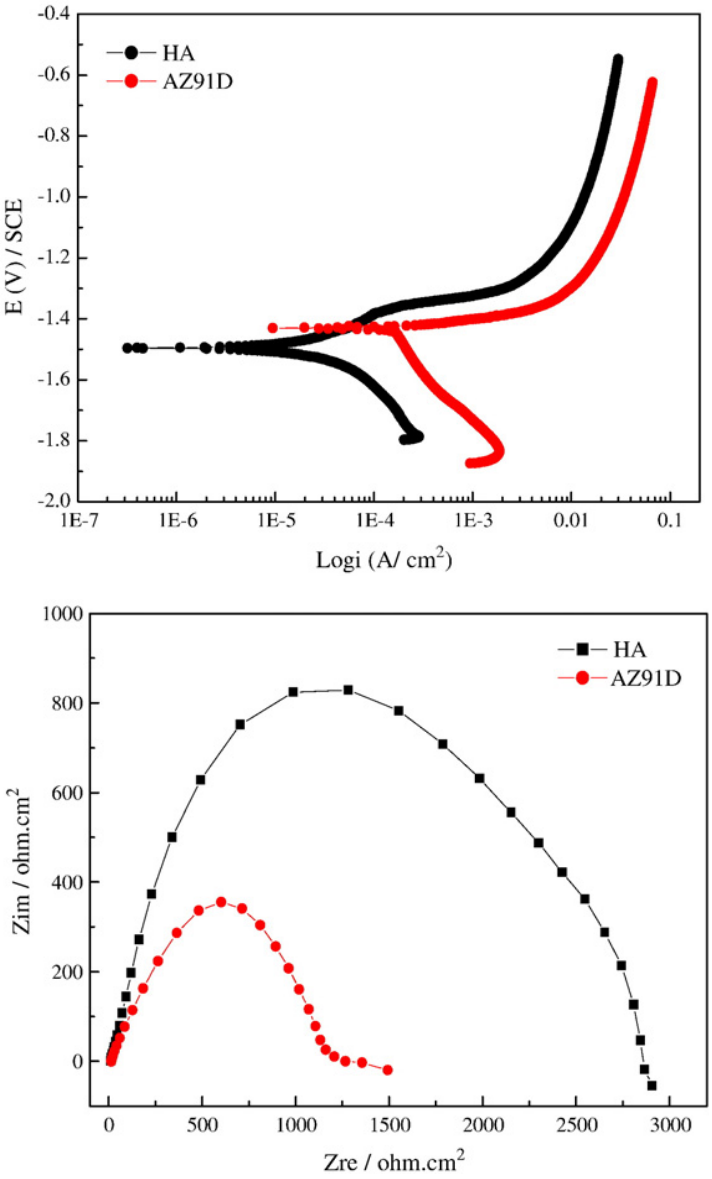

Figure 13. The potentiodynamic curves and EIS plots of magnesium alloy with and without the hydroxyapatite coating in the SBF solution. Reproduced from Song et al. [63] with kind permission.

The biodegradation behaviour of magnesium alloy with and without hydroxyapatite coating by immersion tests in the SBF solution for 48h are shown in Figure 14 [63]. The magnesium alloy substrate suffers serious attack due to the presence of Cl^- in the SBF solution [66]. Plenty of white corrosion products have formed and many cracks can also be observed. The sample with the protection of hydroxyapatite coating only suffers attack to some extent. Parts of the flake-like hydroxyapatite coating have dissolved into the SBF solution. But the corrosion has not penetrated into the coating. The hydroxyapatite coating can continue to protect the magnesium alloy substrate from corrosion for longer time [63].

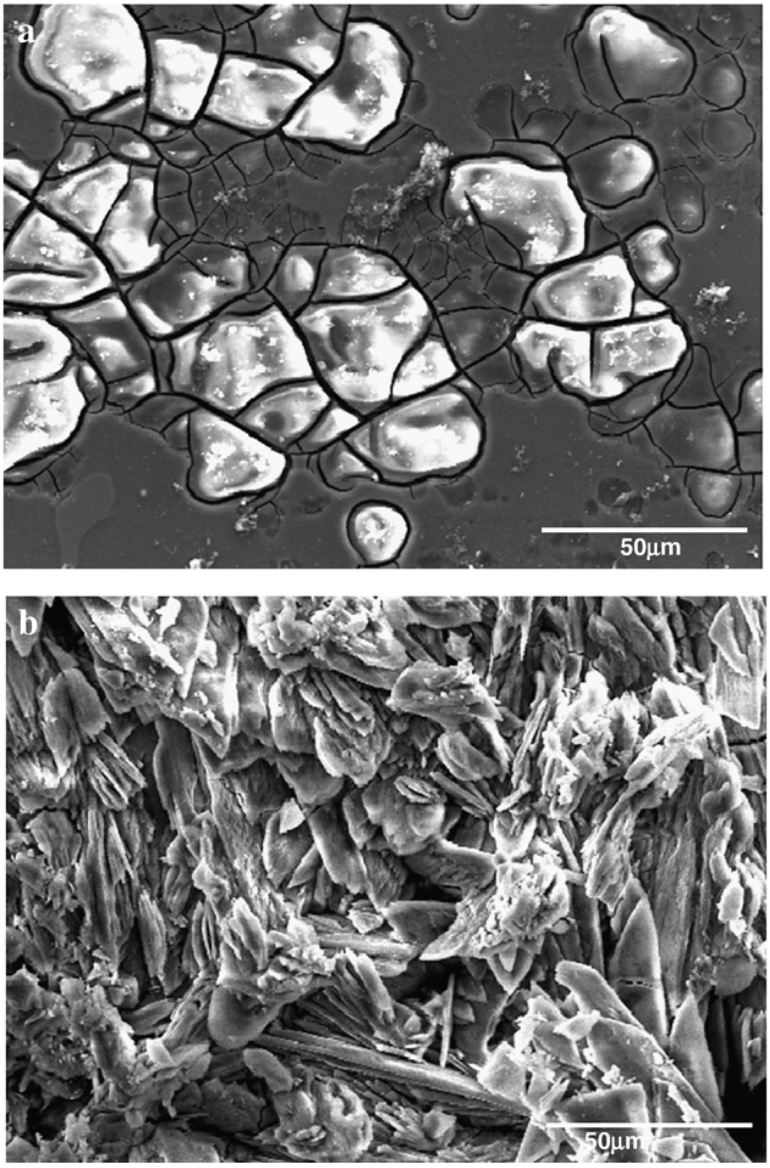

Figure 14. Corrosion morphologies of (a) the magnesium alloy and (b) the hydroxyapatite coating immersed in the SFB solution for 48h. Reproduced from Song et al. [63] with kind permission.

Thus, the hydroxyapatite coating obviously improves the biodegradation rate of magnesium alloys in the SBF solution. The corrosion morphologies also indicate that the hydroxyapatite coating can provides enough protection for biodegradable magnesium alloy substrate [63].

7.2.3. Fluoridated hydroxyapatite (FHA) coating

Recently, fluoridated hydroxyapatite [FHA: $Ca_{10}(PO_4)_6(OH)_{2-2x}F_{2x}$] has been studied as a superior candidate for the substitution of hydroxyapatite in the medical devices [67]. In vitro results have shown that the fluoridated hydroxyapatite can provides lower dissolution, better protein adsorption, and comparable or better cell attachment than the hydroxyapatite and significantly improves alkaline phosphates activity [68]. Also, the fluoridated hydroxyapatite can provides sufficiently low levels of fluoride to acts upon the surrounding cells for improving the bone-like apatite formation [69]. Fluoride ion promotes the mineralization and crystallization of calcium phosphate in the bone formation process [67]. Thus, the fluoridated hydroxyapatite has attracted much attention and has been increasingly investigated as a clinical restoration material due to the extensive findings of that in the bone and teeth and the favourable effects of fluoride ion on the bone growth [69].

Li et al. [57], produced the electrodeposited fluoridated hydroxyapatite coatings with nano-sized crystal bars on the biodegradable magnesium alloy substrate.

The typical SEM images of HBMSC cells on the (A) uncoated and (B) fluoridated hydroxyapatite coated magnesium alloy are shown in Figures 15(A)-(B). It can be seen that after 24h, all cells have spread well on the different surfaces. There are fine filopodia (red circles in Figures 15(A)-(B)) on all groups but more confluences and connections (blue circles in Figure 15(B)) among cells have occurred on the coated group. Typical microscope fields of fluorescence micrographs of the (C) uncoated and (D) fluoridated hydroxyapatite coated magnesium alloy are shown in Figures 15(C)-(D).

These photos show that long red bundles of stress fibers have composed of actin filaments, displaying normal cell cytoskeletons morphology. According to the cell morphology observation, the HBMSC cells have grown and spread well on all groups [57], suggesting the good cell viability [70]. More confluences and connections among cells have occurred on the coated group, which indicate a quicker formation of the cells layers [57].

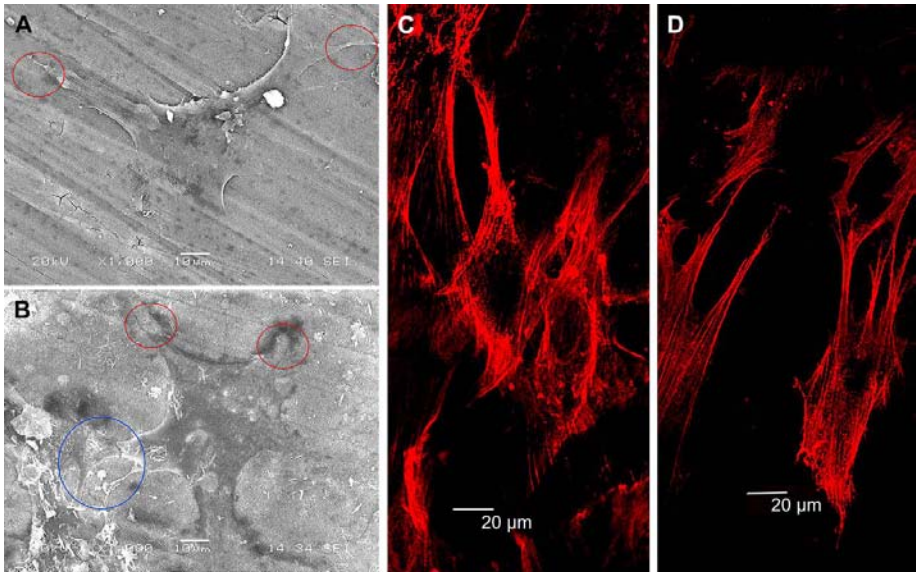

Figure 15. The typical SEM images of HBMSC cells on the (A) uncoated, and (B) fluoridated hydroxyapatite coated magnesium alloy; and the typical microscope fields of fluorescence micrographs of the (C) uncoated, and (D) fluoridated hydroxyapatite coated magnesium alloy. Reproduced from Li et al. [57] with kind permission.

The results of directly proliferated cells on the interface are shown in Figure 16. Noticeably higher absorbance has appeared on the coated group after 2 and 3 days. Based on the data in MTT experiments, a relatively higher OD value indicates that the proliferation proceeds more significantly on the coated samples after 2 and 3 days of incubation [57]. Similarly, more recent studies on the fluoridated hydroxyapatite coatings

have shown the enhanced proliferation of other kinds of cells [69]. Moreover, the appropriate magnesium ions concentration can lead to bone cell activation by regulating the protein synthesis and the ancillary processes [71]. At the same time, the release of calcium ions can benefit osteoblast cell proliferations [72]. Taken together, the existence of fluoride, calcium, magnesium ions, and more stable pH values, can lead to higher proliferation levels for coated group compared to uncoated magnesium alloy [73].

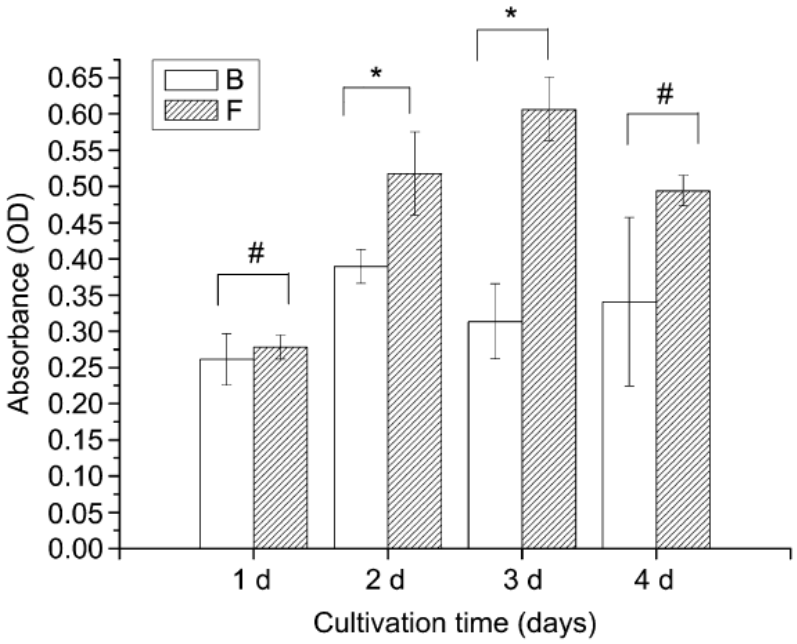

Figure 16. Cells proliferation results according to absorbance values after 1-4 days incubation on the materials ($^{*}p < 0.05$, $\#\, p > 0.05$, 'B' stands for the magnesium alloy group, while 'F' stands for the fluoridated hydroxyapatite coatings group). Reproduced from Li et al. [57] with kind permission.

Thus, by direct cell culture, the bioactive fluoridated hydroxyapatite coated magnesium alloy has presented more stimulation effects to the HBMSC cells proliferation as well as differentiation. Through the molecular biological tests, it could be concluded that the fluoridated hydroxyapatite coatings can regulate the main osteogenic genes after 21 days of the cell culture. In a word, the coated group was more favourable for longer and more stable cell incubation, which manifested the feasibility of a bioactive surface modification method for biodegradable magnesium based alloys [57].

8. Conclusions and Future Research Trends

The practical use of biodegradable magnesium alloys faces the challenge that their biodegradation rates under physiological environments are too fast. This review paper has provided the recent progresses for controlling the biodegradation rate of magnesium alloys.

The amount and distribution of the β phase as a eutectic precipitate, which has been dispersed in matrix, will determine the corrosion performance of the magnesium alloy.

Grain refinement by hot rolling has been shown to lead to a significant reduction in corrosion rate. Hot rolling and grain refinement provide a desirable retardation of corrosion.

The studies indicate that the uncoated sample degraded more rapidly than that of the polymer-coated samples. Although new bone formation is found on both samples, higher volumes of new bone are observed on the polymer-coated samples. The use of polymeric membrane may be potentially applied for future clinical use. The use of bioceramics, which have compounded of calcium and phosphorous ions such as calcium phosphate, hydroxyapatite, and fluoridated hydroxyapatite, as coating for the biodegradable magnesium alloys not only reduce the biodegradation rate of magnesium alloys in the body fluid, but also is useful in constructing the new bone and promoting the osteointegration around the magnesium implants.

The calcium phosphate, hydroxyapatite, and fluoridated hydroxyapatite coatings can significantly decrease the biodegradation rate of magnesium alloy in the body fluid. However, the calcium phosphate coating is highly soluble in the SBF. The hydroxyapatite coating is fragile and easily broken down, and thus the hydroxyapatite coated samples have a higher biodegradation rate than the fluoridated hydroxyapatite coated ones. The hydroxyapatite and the fluoridated hydroxyapatite coatings improve the bioactivity and the mineralization ability of biodegradable magnesium alloy.

In a word, the fluoridated hydroxyapatite coating is a promising coating for biodegradable magnesium alloys as biomaterials.

Decrement of biodegradation rate and increment of bioactivity of magnesium alloys are two prominent factors that many researches have been done on that to improve the degradation properties as well as osteoconductivity of magnesium alloys for future clinical applications.

Future research trends can focus on the following aspects:

The use of other biocompatible elements in the Mg matrix and the assessment of degradation and bioactivity properties and biocompatibility testing for developing of new Mg alloys with biomedical grade.

The use of some new thermomechanical processings for production of nano structured Mg alloy and a comparison between the nano and microstructured Mg alloys for orthopedic applications.

The production of Mg based scaffolds and improvement of degradation properties by bioceramic coating for bone tissue engineering applications.

The use of other bioactive ceramics as coating and reinforcement for the biodegradable magnesium alloys and in vitro and in vivo assessments.

The establish of new standards for in vitro studies of biodegradable magnesium alloys in order to compare the different published results.

And last but not least, the clinically use of modified biodegradable magnesium alloys in the human body for biodegradable bone plates, screws, nails, and bone tissue engineering applications.

Acknowledgement

The author is grateful for support of this research by Isfahan University of Technology.

References

[1] E. J. Lee, S. H. Lee, H. W. Kim, Y. M. Kong and H. E. Kim, Biomater. 26 (2005), 3843-3851.

[2] H. U. Lee, Y. S. Jeong, S. Y. Park, H. G. Kim and C. R. Cho, Curr. Appl. Phys. 9 (2009), 528-533.

[3] Y. Wang, S. Zhang, X. Zeng, L. L. Ma, W. Weng, W. Yan et al., Acta Biomater. 3 (2007), 191-197.

[4] M. Bobby Kannan and R. K. Singh Raman, Scripta Mater. 59 (2008), 175-178.

[5] W. He, E. Zhang and K. Yang, Mater. Sci. Eng. C 30 (2010), 167-174.

[6] S. Zhang, X. Zhang, C. Zhao, J. Li, Y. Song, C. Xie et al., Acta Biomater. 6 (2010), 626-640.

[7] H. Wang, Y. Estrin and Z. Zúberová, Mater. Lett. 62 (2008), 2476-2479.

[8] M. Razavi, M. H. Fathi and M. Meratian, Mater. Charact. 61 (2010), 1363-1370.

[9] M. Razavi, M. H. Fathi and M. Meratian, Mater. Lett. 64 (2010), 2487-2490.

[10] M. Razavi, M. H. Fathi and M. Meratian, Mater. Sci. Eng. A 527 (2010), 6938-6944.

[11] L. Yang and E. Zhang, Mater. Sci. Eng. C 29 (2009), 1691-1696.

[12] M. P. Staiger, A. M. Pietak, J. Huadmai and G. Dias, Biomater. 27 (2006), 1728-1734.

[13] N. Hort, Y. Huang, D. Fechner, M. Störmer, C. Blawert, F. Witte et al., Acta Biomater. 6 (2010), 1714-1725.

[14] M. H. Fathi, M. Meratian and M. Razavi, J. Biomed. Nanotech. 7 (2011), 441-445.

[15] Y. Song, D. Shan, R. Chen, F. Zhang and E. H. Han, Mater. Sci. Eng. C 29 (2009), 1039-1045.

[16] G. Song, Corr. Sci. 49 (2007), 1696-1701.

[17] C. L. Wen, S. K. Guan, L. Peng, C. X. Ren, X. Wang and Z. H. Hu, Appl. Surf. Sci. 255 (2009), 6433-6438.

[18] Y. Xin, C. Liu, K. Huo, G. Tang, X. Tian and P. K. Chu, Surf. Coat. Technol. 203 (2009), 2554-2557.

[19] F. Witte, J. Fischer, J. Nellesen, H. A. Crostack, V. Kaese, A. Pisch et al., Biomater. 27 (2006), 1013-1018.

[20] F. Oktar, M. Yetmez, S. Agathopoulos, T. Goerne, G. Goller, I. Ipeker et al., J. Mater. Sci.: Mater. Med. 17 (2006), 1161-1171.

[21] E. Zhang, L. Yang, J. Xu and H. Chen, Acta Biomater. 6 (2010), 1756-1762.

[22] X. Gu, Y. Zheng, Y. Cheng, S. Zhong and T. Xi, Biomater. 30 (2009), 484-498.

[23] S. Hiromoto, T. Shishido, A. Yamamoto, N. Maruyama, H. Somekawa and T. Mukai, Corr. Sci. 50 (2008), 2906-2913.

[24] Y. Wang, M. Wei and J. Gao, Mater. Sci. Eng. C 29 (2009), 1311-1316.

[25] H. Zreiqat, C. R. Howlett, A. Zannettino, P. Evans, G. Schulze-Tanzil, C. Knabe et al., J. Biomed. Mater. Res. 62 (2002), 175-184.

[26] G. D. Zhang, J. J. Huang, K. Yang, B. C. Zhang and H. J. Ai, Acta Metall. Sin. 43 (2007), 1186-1190.

[27] F. Witte, H. Ulrich, C. Palm and E. Willbold, J. Biomed. Mater. Res. A 81 (2007), 757-765.

[28] R. A. Kaya, H. Cavusoglu, C. Tanik, A. A. Kaya, O. Duygulu, Z. Mutlu et al., J. Neurosurg Spine 6 (2007), 141-149.

[29] R. Waksman, R. Pakala, R. Baffour, D. Hellinga, R. Seabron and F. O. Tio, Circulation 112 (2005), 539-548.

[30] Y. Xin, K. Huo, H. Tao, G. Y. Tang and P. K. Chu, Acta Biomater. 4 (2008), 2008-2015.

[31] F. Witte, I. Abeln, E. Switzer, V. Kaese, A. Meyer-Lindenberg and H. Windhagen, J. Biomed. Mater. Res. A 86 (2008), 1041-1047.

[32] F. Witte, V. Kaese, H. Haferkamp, E. Switzer, A. Meyer-Lindenberg, C. J. Wirth et al., Biomater. 26 (2005), 3557-3563.

[33] Y. Song, S. Zhang, J. Li, C. Zhao and X. Zhang, Acta Biomater. 6 (2010), 1736-1742.

[34] W. C. Kim, J. G. Kim, J. Y. Lee and H. K. Seok, Mater. Lett. 62 (2008), 4146-4148.

[35] S. Zhang, J. Li, Y. Song, C. Zhao, X. Zhang, C. Xie et al., Mater. Sci. Eng. C 29 (2009), 1907-1912.

[36] J. Shi, C. Ding and Y. Wu, Surf. Coat. Technol. 137 (2001), 97-103.

[37] G. Song, Adv. Eng. Mater. 7 (2005), 563-585.

[38] Y. Yun, Z. Dong, D. Yong, M. Schulz and V. Shanov, Mater. Sci. Eng. C 29 (2009), 1814-1821.

[39] A. Gpferich, Biomater. 17 (1996), 103-114.

[40] Y. Wang, C. S. Lim, C. V. Lim, M. S. Yong, E. K. Teo and L. N. Moh, Mater. Sci. Eng. C 31 (2011), 579-587.

[41] S. X. Zhang, X. N. Zhang, C. L. Zhao, J. N. Li, Y. Song, C. Y. Xie et al., Acta Biomater. 6 (2010), 626-640.

[42] Y. Xin, T. Hu and P. K. Chu, Acta Biomater. 7 (2011), 1452-1459.

[43] H. M. Wong, K. Yeung, K. O. Lam, V. Tam, P. K. Chu, K. Luk and K. Cheung, Biomater. 31 (2010), 2084-2096.

[44] R. C. Zeng, W. Dietzel, F. Witte, N. Hort and C. Blawert, Adv. Eng. Mater. 10 (2008), 3-14.

[45] F. Witte, N. Hort, C. Vogt, S. Cohen, K. U. Kainer and R. Willumeit, J. Curr. Opin. in Solid State Mater. Sci. 12 (2008), 63-72.

[46] H. Wang, Y. Estrin, H. Fu, G. Song and Z. Zúberová, Adv. Eng. Mater. 9 (2007), 967-972.

[47] Y. Z. Wan, G. Y. Xiong, H. L. Luo, F. He, Y. Huang and X. S. Zhou, Mater. Des. 29 (2008), 2034-2037.

[48] C. M. Serre, M. Papillard, P. Chavassieux, J. C. Voegel and G. Boivin, J. Biomed. Mater. Res. 42 (1998), 626-633.

[49] Z. J. Li, X. N. Gu, S. Q. Lou and Y. F. Zheng, Biomater. 29 (2008), 1329-1344.

[50] N. T. Kirkland, L. Lespagnol, N. Birbilis and M. P. Staiger, Corr. Sci. 52 (2010), 287-291.

[51] C. Liu, Y. Xin, G. Tang and P. K. Chu, Mater. Sci. Eng. A 456 (2007), 350-357.

[52] J. N. L. P. Cao, X. N. Zhang and S. X. Zhang, J. Mater. Sci. 45 (2010), 6038-6045.

[53] L. Xu, F. Pan, G. Yu, L. Yang, E. Zhang and K. Yang, Biomater. 30 (2009), 1512-1523.

[54] J. Wang, Y. Chao, Q. Wan, Z. Zhu and H. Yu, Acta Biomater. 5 (2009), 1798-1807.

[55] K. Cheng, W. Weng, H. Wang and S. Zhang, Biomater. 26 (2005), 6288-6295.

[56] W. F. Ng, M. H. Wong and F. T. Cheng, Mater. Chemist. Physics 119 (2010), 384-388.

[57] J. Li, Y. Song, S. Zhang, C. Zhao, F. Zhang, X. Zhang, L. Cao, Q. Fan and T. Tang, Biomater. 31 (2010), 5782-5788.

[58] D. Tadic and M. Epple, Biomater. 25 (2004), 987-994.

[59] T. Kokubo and H. Takadama, Biomater. 27 (2006), 2907-2915.

[60] B. Wopenka and J. D. A. Pasteris, Mater. Sci. Eng. C 25 (2005), 131-143.

[61] M. T. Fulmer, I. C. Ison, C. R. Hankermayer, B. R. Constantz and J. Ross, Biomater. 23 (2002), 751-755.

[62] K. A. Bhadang and K. A. Gross, Biomater. 25 (2004), 4935-4945.

[63] Y. W. Song, D. Y. Shan and E. H. Han, Mater. Lett. 62 (2008), 3276-3279.

[64] E. Zhang and L. Yang, Mater. Sci. Eng. A 497 (2008), 111-118.

[65] L. Xu, E. Zhang, D. Yin, S. Zeng and K. Yang, J. Mater. Sci.: Mater. Med. 19 (2008), 1017-1025.

[66] Y. Wan, G. Xiong, H. Luo, F. He, Y. Huang and X. Zhou, Mater. Des. 29 (2008), 2034-2037.

[67] H. Qu and M. Wei, Acta Biomater. 2 (2006), 113-119.

[68] H. Qu, A. L. Vasiliev, M. Aindow and M. Wei, J. Mater. Sci.: Mater. Med. 16 (2005), 447-453.

[69] B. H. Yoon, H. W. Kim, S. H. Lee, C. J. Bae, Y. H. Koh and Y. M. Kong, Biomater. 26 (2005), 2957-2963.

[70] T. Yan, L. Tan, D. Xiong, X. Liu, B. Zhang and K. Yang, Mater. Sci. Eng. C 30 (2010), 740-748.

[71] H. S. Brar, M. O. Platt, M. Sarntinoranont, P. I. Martin and M. V. Manuel, Biomed. Mater. Dev. 61 (2009), 31-34.

[72] G. Ciapetti, E. Cenni, L. Pratelli and A. Pizzoferrato, Biomater. 14 (1993), 359-364.

[73] X. Gu, Y. Zheng, S. Zhong, T. Xi, J. Wang and W. Wang, Biomater. 31 (2010), 1093-1103.

■